Available online at www.sciencedirect.com
SCIENCE DIRECT
Polymer 46 (2005) 3035–3042
polymer
www.elsevier.com/locate/polymer

Tensile yield properties of starch-filled poly(ester amide) materials☆

J.L. Willett[a,*], F.C. Felker[b]

[a]Plant Polymer Research Unit, US Department of Agriculture, Agricultural Research Service, National Center for Agricultural Utilization Research, 1815 North University, 61604-3902 Peoria, IL, USA
[b]Cereal Products and Food Science Research Unit, US Department of Agriculture, Agricultural Research Service, National Center for Agricultural Utilization Research, 1815 North University, 61604-3902 Peoria, IL, USA

Received 22 October 2004; received in revised form 16 December 2004; accepted 28 January 2005
Available online 8 March 2005

Abstract

Composite materials were prepared with granular corn starch (CS) or potato starch (PS) and poly(ester amide) resin (PEA), with starch volume fractions (ϕ) up to 0.40. Tensile yield properties were evaluated at strain rates of 0.0017–0.05 s^{-1}. Yield stress of the CS-PEA materials increased with strain rate and starch content. The strain rate effect became more pronounced as the starch content increased. A crossover effect was observed with PS-PEA materials: at low strain rates, the yield stress decreased with increasing ϕ, and increased with ϕ at higher strain rates. This crossover suggests that the time scale of debonding in the PS-PEA materials is comparable to the time scale of the tension test. The addition of either CS or PS to PEA induced a distinct maximum in the stress–strain curve at yield compared to the neat PEA. Debonding of starch granules from the PEA matrix occurred at lower stresses in the PS-PEA materials than the CS-PEA. In PS-PEA, debonding occurred in bands similar in appearance to shear bands throughout the tensile specimen. After yielding, the cross-section area decreased as the debonded zones coalesced. In the CS-PEA materials, debonding zones were more diffuse, and a distinct neck formed at yield. Yield stress data for the CS-PEA materials could be shifted with respect to strain rate to construct a master curve, indicating that yield properties at these strain rates were determined by the matrix response rather than debonding as observed in other starch-filled materials.

Keywords: Starch; Composites; Fillers

1. Introduction

Growing concerns over the environmental impact of solid waste disposal have increased interest in biodegradable polymers in recent years. While a number of biodegradable polymers, particularly polyesters, have been developed, their commercial success has often been limited in part due to their high cost relative to commodity thermoplastics. Because of its low cost, biodegradability, and renewability, starch has been investigated as a filler and extender for many of these polymers.

A general difficulty encountered in the use of granular starch as a filler and extender is the reduction in yield and tensile strength as starch content is increased. When starch is added to polycaprolactone (PCL), yield and tensile strength decrease as starch content increases [1–3]. Scanning electron micrographs show extensive debonding and void elongation in these materials. Comparable results have been reported for starch-filled polyhydroxyalkanoates (PHAs) [1,4,5]. Shogren reported improvement in tensile strength of starch-filled PHA by precoating the starch with poly(ethylene oxide) [6], while Willett et al. reported improvements in tensile strength by grafting poly(glycidyl methacrylate) to the starch granules [7]. Reductions in strength were also observed with starch-filled poly(butylene succinate adipate) [8] and poly(lactic acid) (PLA) [9]. Garlotta et al. reported reductions in tensile strength for starch-filled PLA, although moderate increases were found in ternary starch-PLA-poly(hydroxyester ether) composites for starch contents up to approximately 30 wt% [10].

Another class of biodegradable polymers are the poly(ester amide)s introduced by Bayer [11]. Ferre et al. reported that adding starch (20 wt%) to PEA reduced the

☆Names are necessary to report factually on available data; however, the USDA neither guarantees nor warrants the standard of the product, and the use of the name by USDA implies no approval of the product to the exclusion of others that may also be suitable.

* Corresponding author.
E-mail address: willetjl@ncaur.usda.gov (J.L. Willett).

0032-3861/$ - see front matter © 2005 Elsevier Ltd. All rights reserved.
doi:10.1016/j.polymer.2005.01.059

tensile strength by approximately 40% [12]. While cryo-fractured samples showed some adherence of PEA to starch granules, extensive debonding and void elongation were observed in strained samples. Averous et al. described thermoplastic starch-PEA blends in which the PEA was the minor phase (25 or 40 wt%), and reported that starch-PEA blends had 'better interphase compatibility' compared to other biodegradable polymers they investigated [13]. Coextruded films of thermoplastic starch with poly(ester amide) have also been reported in which interfacial strength was improved due to mechanical interlocking between adjacent layers [14].

Little has been reported of the effect of strain rate on tensile properties of starch-filled polymers, or of the effect of starch type on properties of starch-PEA materials. We report here the tensile yield properties of PEA blended with granular corn starch or potato starch over a range of strain rates at room temperature.

2. Experimental

2.1. Materials

Unmodified corn starch (CS) (Pure Food Powder, Tate&Lyle, Decatur, IL) and potato starch (PS) (Avebe America, Princeton, NJ) were used. Starches were dried to less than 0.5% moisture content before processing. CS granule diameters ranged from approximately 5–25 μm, with an average diameter of 16.1 μm, while the PS diameters ranged from approximately 15–70 μm with an average diameter of 30.1 μm [15] consistent with other data for these starch types [16]. Poly(ester amide) (PEA) resin denoted BAK 404-004 was provided by Bayer Corporation (Pittsburgh, PA). This PEA is derived from Nylon 6, and has a melting point of 125 °C.

2.2. Processing

Starch-PEA materials were formulated with volume fractions of starch of 0.05, 0.13, 0.21, and 0.40, corresponding to weight fractions of 0.06, 0.14, 0.23, and 0.43. Controls with no starch were also prepared. All materials were prepared by extrusion compounding using a Werner-Pfleiderer ZSK-30 twin screw extruder (Coperion Corp., Ramsey, NJ). The PEA resin was fed into the extruder and melted in a series of kneading blocks. Starch was fed downstream at $L/D=22$, and the two components were mixed in another series of kneading blocks. Strands were air cooled and chopped into pellets for injection molding. Total feed rate was 90 g/min, screw speed was 200 rpm, and the temperature profile over the eight controls zones of the extruder were 27 (feed)/93/93/177/177/163/149/135 °C. Melt temperature at the die was 135 °C. Test specimens (ASTM D 638 type I) were prepared using a Cincinnati Milacron ACT model injection molding machine. Barrel and sprue temperatures were 180 °C with a mold temperature of 50 °C.

2.3. Tensile measurements

Molded test specimens were conditioned 24 h at 50% relative humidity and 22 °C before testing. Tensile measurements (gage length 50 mm) were performed using an Instron 4201 Universal Load Frame at crosshead speeds of 5, 15, 50, and 150 mm/min, corresponding to nominal strain rates of 0.0017, 0.0051, 0.0167, and 0.051 s^{-1}. Three to five specimens were tested for each formulation. Yield stress and yield strain were defined at the point where the stress–strain slope was zero; modulus values were determined using the instrument software from the initial portion of the stress–strain curves. Testing was terminated at $\varepsilon \approx 1$ for all samples except $\phi = 0.40$, which failed immediately after yielding.

2.4. Scanning electron microscopy

Samples for SEM analysis were cooled in liquid nitrogen and cryogenically fractured. Fracture planes were prepared parallel to the tensile loading axis across the sample thickness direction. After sputter coating with Au–Pd, samples were viewed in a JEOL 6400V scanning electron microscope.

3. Results and discussion

Stress–strain (σ–ε) curves are shown for CS-PEA and PS-PEA materials at strain rates of 0.0017 s^{-1} (Fig. 1) and 0.0167 s^{-1} (Fig. 2) and starch volume fractions (ϕ) of 0, 0.21, and 0.40. For the unfilled PEA at the lowest strain rate, no maximum stress was seen, and no distinct yield stress could be determined using a Considere plot (data not shown). At the higher strain rates, broad maxima were observed in the stress–strain curves of the unfilled PEA with little strain softening. Distinct necking was not observed in the unfilled PEA at any strain rate used, indicating that the unfilled PEA deformed in a quasi-homogeneous manner at these strain rates.

The starch-filled PEA materials display a distinct maximum stress at all filler contents and strain rates studied. Addition of corn starch to PEA increased σ_y at all strain rates used. Except when $\phi = 0.40$, the starch-filled materials could be extensively drawn after yielding. After yielding, stress in the starch-filled materials decreased until a stable draw stress (σ_d) was reached. The draw stress for CS-PEA was slightly greater than that of the unfilled PEA, while for the PS-PEA σ_d was lower. This suggests that the PEA yielded prior to debonding in the CS-PEA materials, followed by strain hardening which increased the draw stress. The reduction in stress (strain softening) in the CS-PEA was accompanied by the formation of a distinct neck

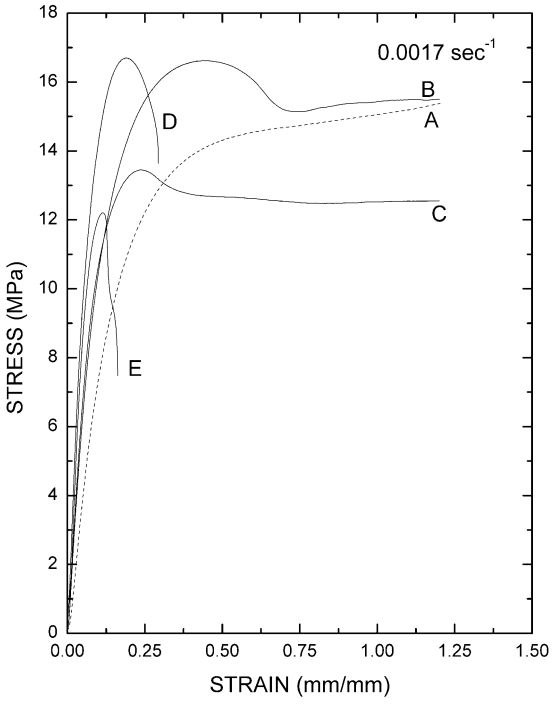

Fig. 1. Stress–strain curves for starch-PEA materials at strain rate 0.0017 s^{-1}. (a) PEA control; (b) CS-PEA ($\phi=0.21$); (c) PS-PEA ($\phi=0.21$); (d) CS-PEA ($\phi=0.40$); (e) PS-PEA ($\phi=0.40$).

(discussed below) and intense whitening in the neck region. This suggests the reduction in stress after yielding was due largely to the onset of debonding in the CS-PEA. Compared to the PS-PEA materials, yield peaks for the CS-PEA materials were broader, and the stress reductions $\Delta\sigma=\sigma_y-\sigma_d$ were larger. At the lower strain rates, σ_y values for the PS-PEA materials decreased for $\phi>0.06$, while at higher strain rates σ_y increased over the entire ϕ range.

As shown in Fig. 3 for strain rates of 0.0017 and 0.051 s^{-1} σ_y for the CS-PEA is greater than that of the PS-PEA for ϕ greater than 0.06. For both starch types, the yield stress values significantly exceed predictions of the Nicolais–Narkis model [17]:

$$\sigma_{y,f} = \sigma_{y,0}(1 - 1.21\phi^{2/3}) \quad (1)$$

where subscripts f and 0 denote filled and unfilled. Eq. (1), which assumes complete debonding between matrix and filler, predicts a monotonic decrease in σ_y with increasing filler content due to the reduction in effective cross-sectional area and is often used to model the yield strength of filled polymers. Fig. 3 shows significant increases in yield stress for the starch-filled PEA, in contrast to the reductions in yield stress or tensile strength reported for many starch-filled materials (see Section 1). Figs. 1–3 imply more debonding in PS-PEA than CS-PEA prior to yield, particularly at lower strain rates.

From Figs. 1–3, it is clear that the starch phase in the CS-PEA materials carries a portion of the stress prior to yielding. In the absence of debonding, yielding occurs when the stress in the PEA matrix (σ_m) reaches $\sigma_{y,0}$. Using the approach of Pukanszky [18], we can write

$$\sigma_e = \phi k \sigma_e + (1 - \phi)\sigma_m \quad (2)$$

where σ_e is the external (macroscopic) stress and k is a

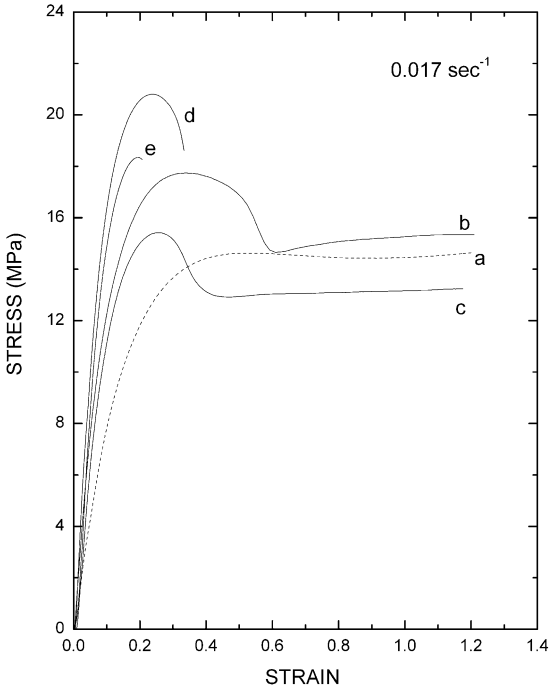

Fig. 2. Stress–strain curves for starch-PEA materials at strain rate 0.017 s^{-1}. (a) PEA control; (b) CS-PEA ($\phi=0.21$); (c) PS-PEA ($\phi=0.21$); (d) CS-PEA ($\phi=0.40$); (e) PS-PEA ($\phi=0.40$).

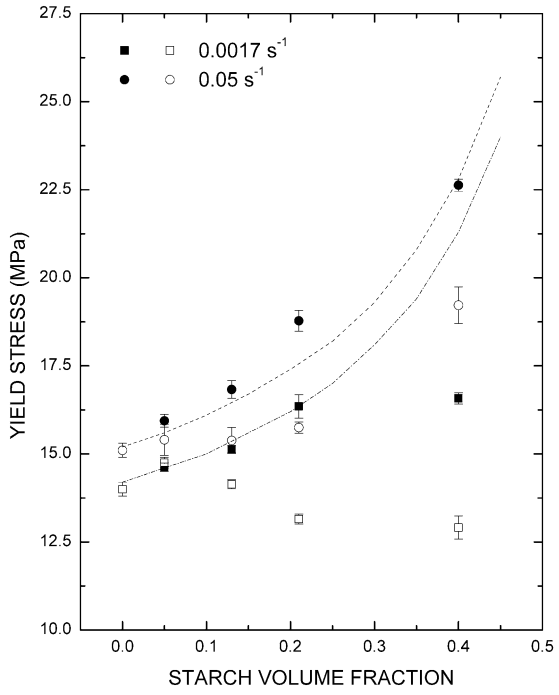

Fig. 3. Yield stress dependence on starch volume fraction for CS-PEA (filled symbols) and PS-PEA (open symbols). Strain rates are 0.0017 and 0.051 s^{-1}. Lines are drawn using Eq. (3) with $k=1.4$.

measure of the stress transfer to the filler (starch) phase. The external stress required to induce matrix yielding is obtained by setting $\sigma_m = \sigma_{y,0}$ and rearranging Eq. (2):

$$\sigma_e = \sigma_{y,0} \frac{1-\phi}{1-k\phi} \tag{3}$$

Eq. (3) predicts an increase in yield stress when $k > 1$. Analysis of the CS-PEA data gives $k \approx 1.4$, independent of strain rate. As seen in Fig. 3, Eq. (3) adequately describes the CS-PEA data over the entire ϕ range at the highest strain rate, as well as the data up to $\phi = 0.21$ at the lowest strain rate. Similar results are obtained for the other two strain rates as well (data not shown). Eq. (3) does not describe the PS-PEA data, due to debonding prior to yield (see below).

Modulus data are shown in Fig. 4. For both CS-PEA and PS-PEA, the modulus increases monotonically with starch volume fraction. Differences between the two starch types are not significant. Also plotted in Fig. 4 is the prediction of the Kerner equation [19]:

$$E = E_0 \left(1 + \frac{15(1-\nu)}{8-10\nu} \frac{\phi}{1-\phi}\right) \tag{4}$$

where ν is Poisson's ratio, taken to be equal to that of polyethylene (0.43), and E_0 is the modulus of the PEA. The solid line in Fig. 4 uses the PEA modulus value at the highest strain rate, while the dotted line uses the PEA modulus at the lowest rate. It is observed that the Kerner equation adequately describes the moduli of both CS-PEA and PS-PEA over the entire range of starch content, although the predicted values are somewhat lower than the measured values at the highest starch content. This fit implies that the starch modulus is much greater than the PEA modulus, consistent with reported values of 15 GPa [20] and 5.2 GPa [21]. There is no significant dependence of the modulus values on strain rate for either CS-PEA or PS-PEA materials. Modulus values were measured at strains of 0.05 or less; the equivalent modulus values for PS-PEA and CS-PEA imply little if any debonding in the initial stages of tensile loading.

Yield strain (ε_y) data are shown in Fig. 5. Yield strain monotonically decreases with increasing ϕ. At all starch contents, the PS-PEA materials have lower ε_y values than the CS-PEA materials at a given strain rate. Yield strains are greater than those predicted using the Nielsen model for filled materials [19]:

$$\varepsilon_f = \varepsilon_0 (1 - \phi^{1/3}) \tag{5}$$

where f and 0 denote filled and unfilled as in Eq. (1).

The increases in yield stress shown in Figs. 1–3 imply stress transfer to the starch phase prior to yielding. Only at the lowest strain rates does σ_y decrease, and only for the PS-filled PEA. These results suggest a viscoelastic debonding process with a time scale comparable to or greater than that of tensile loading. To clarify debonding in these materials, samples were loaded to various stress levels, removed from the grips, and observed using a back-lighting method. This approach has been show to be useful in characterizing debonding in starch-filled materials [22]. Fig. 6(A) and (B) show samples ($\phi = 0.21$) which were loaded to a stress of

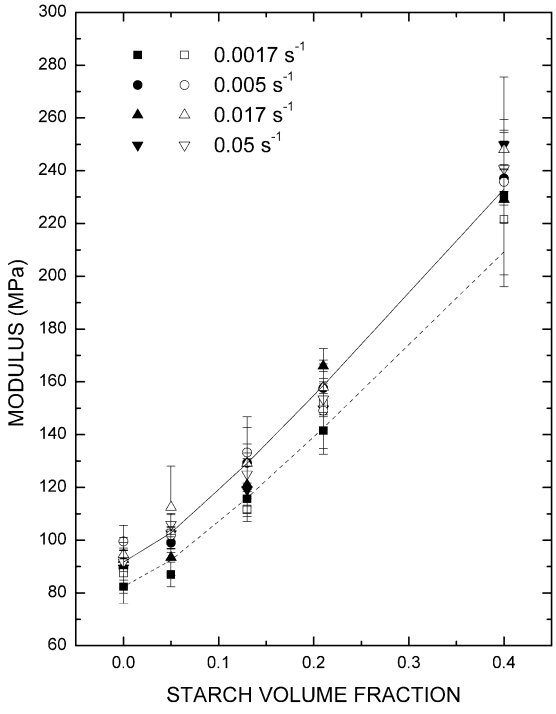

Fig. 4. Modulus dependence on starch volume fraction for CS-PEA (filled symbols) and PSPEA (open symbols). The curves are drawn using the Kerner equation (Eq. (4)).

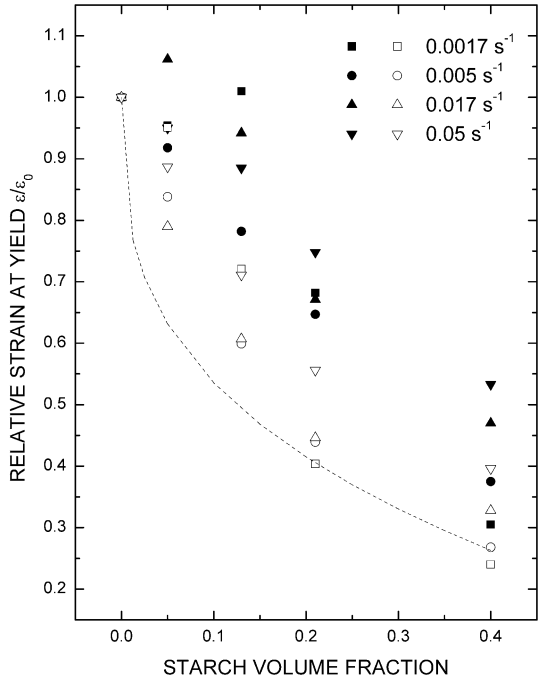

Fig. 5. Yield strain dependence on starch volume fraction for CS-PEA (filled symbols) and PS-PEA (open symbols) materials. The curve is the model prediction using Eq. (5).

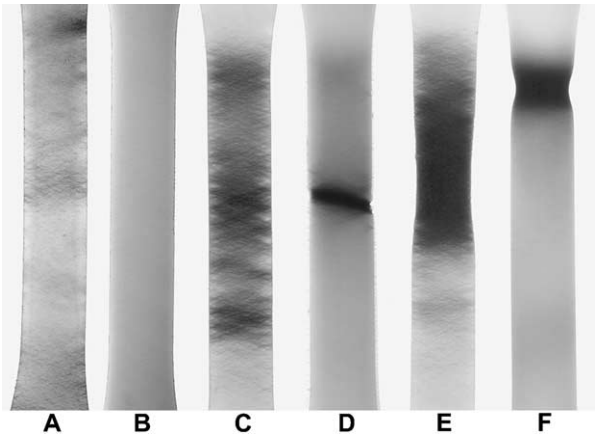

Fig. 6. Visualization of debonding in PS-PEA (A,C,E) and CS-PEA (B,D,F). Starch volume fraction = 0.21. Test conditions are described in the text.

12.5 MPa at a rate of 0.0017 s^{-1}, then released. This stress is less than the maximum stress for the filled materials, and well below the PEA yield stress of 14.0 MPa (see Fig. 1). Debonded zones, visible as dark bands, are uniformly dispersed throughout the PS-PEA sample, while little if any debonding is visible in the CS-PEA sample. Therefore, it appears that the reduction in yield stress seen in the PS-PEA materials is due to debonding prior to yield. The increased pre-yield debonding in the PS-PEA materials is consistent with the lower $\Delta\sigma$ values discussed above (Figs. 1 and 2).

Fig. 6(C) and (D) show samples which were loaded past yield at the same strain rate. Debonded zones, oriented at an angle of approximately 68° to the tensile axis, are obvious throughout the gage length of the PS-PEA sample. Although this sample has been extended past the yield point, no distinct neck is yet visible; the cross section area reduction is less than 2%. Debonded zones are also visible in the CS-PEA sample, although the band structure is not as apparent. A well-defined neck region has formed in this sample, with a cross section area reduction of approximately 25%. The neck is oriented at the same angle as the debonding zones seen in the PS-PEA sample. The neck region shows intense stress whitening due to debonding and elongation of voids. As shown below, debonding is complete inside the neck region of the CS-PEA samples.

Fig. 6(E) and (F) show samples loaded past yield at 0.0167 s^{-1}. In both samples, a neck region of reduced cross section area has formed. The PS-PEA sample displays debonding zones similar to those seen at the lower strain rate, which have coalesced into a neck region after yielding. The CS-PEA sample is similar in appearance to the sample loaded at 0.0017 s^{-1}, with debonding zones concentrated around a distinct neck. In each sample, the cross section area is reduced about 35% relative to the unstretched samples. The neck in the CS-PEA samples, with intense stress whitening and area reduction, grew in length as samples were stretched past the yield point while maintaining a sharp boundary with the undrawn portion of the sample. The transition into the neck region of the PS-PEA sample was less well-defined in comparison and did not grow by the mechanism seen in CS-PEA.

When $\phi = 0.40$, PS-PEA and CS-PEA samples failed immediately after yielding without drawing (see Figs. 1 and 2). Stress whitening was concentrated in the zone immediately adjacent to the fracture plane. The transition to a quasi-brittle fracture mode indicates that the stress in the PEA matrix after debonding exceeds its ultimate strength. According to the model of Bazhenov et al. [23], quasi-brittle fracture in filled ductile polymers occurs above a critical filler volume fraction determined by the degree of strain-hardening in the unfilled matrix. Preliminary results suggests the critical volume fraction for PEA is approximately 0.30, as PS-PEA samples with $\phi = 0.33$ failed immediately after yield, while samples with $\phi = 0.27$ could be drawn after yield (data not shown).

Fig. 7 shows scanning electron micrographs of samples with $\phi = 0.21$ loaded at a strain rate of 0.0167 s^{-1} past the yield point. The fracture surfaces are cross-sections of the sample thickness (parallel to the tensile axis and perpendicular to the tensile fracture plane) and were prepared by cryogenically fracturing samples. In Fig. 7(A) (CS-PEA) and (D) (PS-PEA), taken from outside the neck region, some debonding is visible, but it is apparent that not all granules have debonded in this region. Fig. 7(B) and (E) show similar views taken from regions closer to the neck. Many granules have debonded, and voids are visible around the granules. Fig. 7(C) and (F) are taken from the neck regions. All granules are debonded, and significant void extension is seen. The voids shown in Fig. 7(C) and (F) are presumably

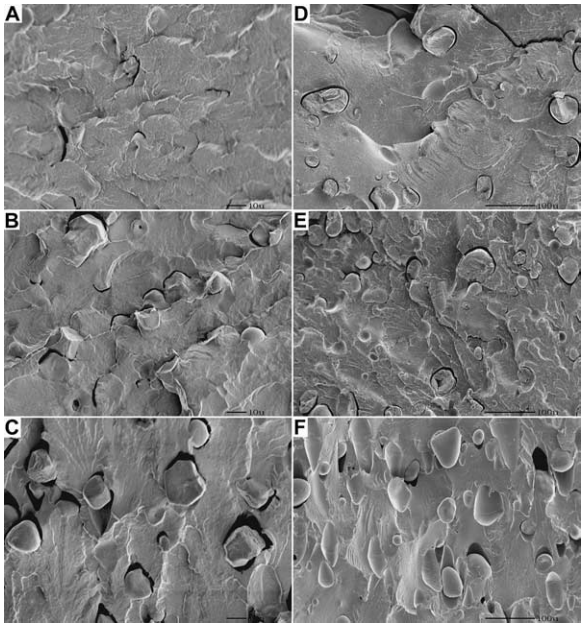

Fig. 7. Scanning electron micrographs of CS-PEA (A,B,C) and PS-PEA (D,E,F) samples after loading at 0.0167 s^{-1}. Surfaces are thickness cross-sections parallel to the tensile axis and perpendicular to the tensile fracture plane. Tensile axis is vertical. Magnification is 1000× for A–C and 250× for D–F. Starch volume fraction = 0.21.

larger when the samples are under tension; the stretched samples retracted several millimeters when the load was removed. These images suggest the stress required for debonding in the CS-PEA is of the same order of magnitude as the yield stress at the strain rates used in this work, while debonding stresses for PS-PEA are somewhat lower.

Few direct measurements of starch-polymer adhesion are available in the literature. Using surface energies, Biresaw estimated the work of adhesion (W_a) between starch and various biodegradable polyesters, including PCL and PHA, to be approximately 0.08 N/m [24]. This value can be compared to the work required to create surface area (γ) during debonding in starch-filled PEA. Debonding will occur when the stored elastic energy (U_{el}) exceeds the energy required to create the free surface of the starch granule and the surface of the polymer cavity (W_{db}). These two energy terms may be written as follows:

$$U_{el} = \frac{\sigma^2 V}{2E} \tag{6a}$$

$$W_{db} = 2 \times 4\pi\gamma R^2 \tag{6b}$$

Setting $V=(4\pi/3)R^3$ and $U_{el}=W_{db}$ gives

$$\sigma_{db} = \frac{1}{S}\left(\frac{12E\gamma}{R}\right)^{1/2} \tag{7}$$

E is the elastic modulus and R is the (starch) particle radius. For rigid spherical particles in a softer matrix, the stress at the particle pole is intensified by a factor $S \approx 2$ [25]. Eq. (7), therefore, gives the macroscopic stress at which debonding is expected to occur. A similar relationship has been reported by Chow [26]. For the CS-PEA, $E \approx 150$ MPa (Fig. 4) and R is approximately 8×10^{-6} m for corn starch. Using the W_a value determined by Biresaw [24] in Eq. (7) gives a debonding stress of approximately 2.2 MPa. This value is clearly too low for the CS-PEA under these conditions, as shown by the lack of debonding in Fig. 6 at stresses up to 12 MPa. On the other hand, a debonding stress of 16 MPa (CS-PEA, Fig. 1) gives $\gamma \approx 4$ J/m^2. Consistent with the data of Figs. 1, 2, and 6, Eq. (7) predicts a lower debonding stress for PS-PEA due to the larger particle size of potato starch (15×10^{-6} m). The fact that γ exceeds estimates of W_a by two orders of magnitude reflects the dominant role of viscoelastic effects in debonding, which are neglected in the derivation of Eq. (7). Gent and Kinloch have demonstrated that failure energy of viscoelastic materials bonded to rigid substrates is composed of a reversible work of adsorption, corresponding to W_a, and an irreversible work of deformation during separation; the irreversible component increases with increasing rate [27].

Yield stresses are plotted against strain rate for CS-PEA and PS-PEA materials in Fig. 8 using an Eyring-type plot. The slope of the neat PEA data gives an estimated activation volume of approximately 7.4×10^{-3} m^3/mol, which is comparable to that for many thermoplastics [28]. As seen

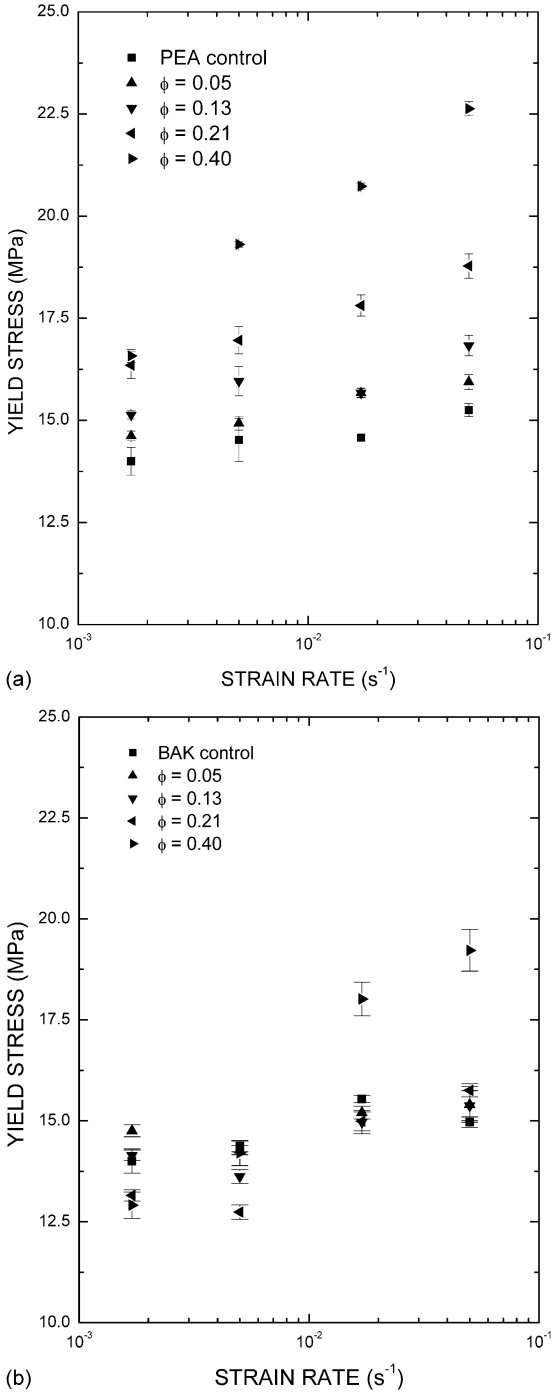

Fig. 8. Yield stress as a function of strain rate for CS-PEA (a) and PS-PEA (b).

in Fig. 8(a), σ_y increases with strain rate and starch content for the CS-PEA materials. The rate effect is more pronounced at higher starch contents, with σ_y ($\phi=0.40$) approximately 50% greater than σ_y of the neat PEA resin at the highest strain rate. In general, addition of a rigid filler reduces the tensile yield stress of thermoplastics due to debonding effects if the average particle size is greater than approximately one micrometer. Reinforcement (increased

yield strength) typically requires particle sizes much less than the sizes of the starch granules in this work. The increases in σ_y in the CS-filled PEA are in contrast to the reductions observed in other starch-filled materials.

In the PS-PEA materials, σ_y decreases as ϕ increases at low strain rates, as shown in Fig. 8(b). At higher strain rates, σ_y for the PS-PEA is greater than that for the unfilled PEA, with the effect most pronounced at $\phi = 0.40$. Below a critical strain rate of approximately $10^{-2}\ s^{-1}$, debonding leads to a reduction in yield stress. At higher strain rates, debonding is reduced and reinforcement is observed similar to that in the CS-PEA materials.

Fig. 8(a) suggests that below a critical strain rate of approximately $10^{-5}\ s^{-1}$, σ_y for the CS-PEA will drop below that of the neat PEA. The time scale for debonding in CS-PEA at the test temperature (22 °C) is, therefore, approximately three orders of magnitude greater than that in the PS-PEA. The reason for this difference is not clear but may be related to particle size or to interphase effects [18]. The effect of temperature on critical strain rate was not characterized.

The CS-PEA yield stress data in Fig. 8(a) can be shifted to construct a master curve as shown in Fig. 9. The data for $\phi \leq 0.40$ appear to fall on a smooth curve when shifted by an appropriate factor. The shifted data cover four orders of magnitude in strain rate compared to the factor of 30 in Fig. 8. The data for $\phi = 0.40$, especially at the lowest test rate, do not fit the master curve as well. As seen in Figs. 1 and 2, this starch content failed at much lower strains than lower starch contents, immediately past the yield point, whereas CS-PEA materials with lower starch contents could be drawn to much higher strains. The lowest (shifted) strain rates in Fig. 9 are approximately equal to critical strain rate discussed above; the CS-PEA master curve is valid only for strain rates above the critical value for debonding. The PS-PEA data cannot be shifted to construct a master curve, although it is anticipated that a master curve could be constructed for strain rates exceeding the critical rate.

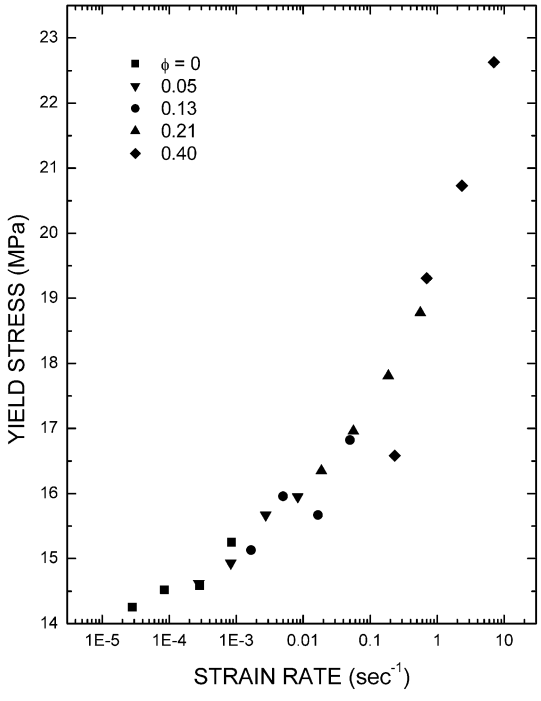

Fig. 9. Master curve for CS-PEA yield stress at 22 °C. Reference curve is $\phi = 0.13$.

The CS-PEA results of Figs. 8 and 9 are similar to those reported by Sumita et al. [29] for glass-filled polypropylene (up to 20 wt% filler), who constructed master curves by shifting yield stress data with respect to temperature, strain rate, and filler content for particle sizes in the range of 7–40 nm. The physical effect of adding reinforcing particles was to shift the material response to that expected for the matrix at either higher strain rates or lower temperatures. The ability to shift the yield stress data with respect to filler content implies that yielding is dominated by the matrix properties, consistent with Eq. (3). In contrast, yield in many filled semi-crystalline polymers is dominated by particle-matrix debonding [30–34]. It is noteworthy that the corn starch, with a particle size range of 5–25 μm, can act as a reinforcing agent in PEA, whereas particle sizes in the nanometer range are required for glass bead reinforcement of polypropylene [29].

It is clear from Figs. 3, 6, and 8 that there are significant differences in the tensile properties of PS-PEA compared to CS-PEA. These differences may be due primarily to particle size effects. Eq. (7) and similar relations [26] predict an effect on the order of $(R_{CS}/R_{PS})^{1/2} \approx (8/15)^{1/2} \approx 0.7$. If the PS-PEA properties are dominated by the effects of the larger particle fraction, then this effect may be on the order of ≈ 0.5. Debonding differences may also be sensitive to the chemical nature of the starch granule surfaces. CS has a higher protein content (0.14% N) than PS (0.05% N); if CS has a greater protein content on the granule surface then the CS-PEA interactions may be quite different than those in PS-PEA. In addition, native PS contains charged phosphate groups, although it is not clear what effect if any phosphate groups would have on starch-PEA interactions. Differences in particle shape may also impact debonding; CS granules are roughly spherical with many faceted granules present, while PS granules are typically smooth and ellipsoidal with aspect ratios of approximately 1.5 [35].

4. Summary

The tensile yield properties of starch-filled poly(ester amide) were measured at various starch contents and strain rates. Yield stress increased relative to the unfilled PEA with starch volume fraction ϕ and strain rate when corn starch was the filler. When potato starch was used, the yield stress decreased with ϕ at low strain rates, and increased at high strain rates. CS-PEA yield stress data were shifted to construct a master curve at the test temperature covering four orders of magnitude in strain rate, whereas the PS-PEA

data could not be shifted. The increases in yield stress of the starch-filled PEA are in contrast to the decreases typically observed in other starch-filled polymers.

Acknowledgements

The authors acknowledge the assistance of B. Jasberg, R.P. Westhoff, G.D. Grose, and Dr A.R. Thompson (SEM micrographs), and useful comments provided by Dr Sterling St. Lawrence.

References

[1] Koenig MF, Huang SJ. Polymer 1995;36:1877–82.
[2] Pranamuda H, Tokiwa Y, Tanaka K. J Environ Polym Degrad 1996;4: 1–7.
[3] Odusanya OS, Ishiaku US, Azemi BMN, Manan BDM, Kammer HW. Polym Eng Sci 2000;40(6):1298–305.
[4] Ramsay BA, Langlade V, Carreau PJ, Ramsay JA. Appl Environ Micro 1993;59:1242–6.
[5] Kotnis MA, O'Brien GS, Willett JL. J Environ Polym Deg 1995;3: 97–105.
[6] Shogren RL. J Environ Polym Degrad 1995;3:75–80.
[7] Willett JL, Kotnis MA, O'Brien GS, Fanta GF, Gordon SH. J Appl Polym Sci 1998;70:1121–7.
[8] Ratto JA, Stenhouse PJ, Auerbach M, Mitchell J, Farrell R. Polymer 1999;40:6777–88.
[9] Ke T, Sun X. Cer Chem 2000;77(6):761–8.
[10] Garlotta D, Doane WM, Shogren RL, Lawton JW, Willett JL. J Appl Polym Sci 2003;88:1775–86.
[11] Grigat E, Koch R, Timmermen R. Polym Degrad Stab 1998;59:223–6.
[12] Ferre T, Franco L, Rodrigues-Galan A, Puiggali J. Polymer 2003;44: 6139–52.
[13] Averous L, Fringant C. Polym Eng Sci 2001;41:727–34.
[14] Martin O, Averous L. J Appl Polym Sci 2002;86:2586–600.
[15] Zhou G, Willett JL, Carriere CJ, Wu YV. J Polym Environ 2002;8: 145–50.
[16] Snyder EM. Industrial microscopy of starches. In: Whistler RL, Bemiller JN, Paschall EF, editors. Starch chemistry and technology. Orlando: Academic Press; 1984. p. 661–74.
[17] Nicolais L, Narkis M. Polym Eng Sci 1971;11:194–9.
[18] Pukanszky B, Voros G. Polym Comp 1996;17:384–92.
[19] Nielsen LE, Landel RF. Mechanical properties of polymers and composites. 2nd ed. New York: Marcel Dekker; 1994.
[20] Willett JL. J Appl Polym Sci 1994;54:1685–95.
[21] Owen AJ, Koller I. Polymer 1996;37:527–30.
[22] St. Lawrence S, Walia PS, Felker FC, Willett JL. Polym Eng Sci 2004; 44:1839–47.
[23] Bazhenov S, Li JX, Hiltner A, Baer E. J Appl Polym Sci 1994;52: 243–54.
[24] Biresaw G, Carriere CJ. J Polym Sci, Part B 2001;39:920–30.
[25] Goodier JN. Appl Mech 1933;55:39–44.
[26] Chow TS. J Polym Sci, Polym Phys Ed 1982;20:2103–9.
[27] Gent AN, Kinloch AJ. J Polym Sci A-2 1971;9:659–68.
[28] Ward IM, Hadley DW. An introduction to the mechanical properties of solid polymers. New York: Wiley; 1993.
[29] Sumita M, Tsukumo Y, Miyasaka K, Ishikawa KJ. Mater Sci 1983;18: 1758–64.
[30] Kim GM, Michler GH, Galan LJ, Fiechter AJ. Appl Polym Sci 1996; 60:1391–403.
[31] Meddad A, Fisa B. J Appl Polym Sci 1997;65:2013–24.
[32] Dubnikova IL, Oshmyan VG, Gorenberg AY. J Mater Sci 1997;32: 1613–22.
[33] Suwanprateeb J, Tiemprateeb S, Kangwantrakool S, Hemachandra K. J Appl Polym Sci 1998;70:1717–24.
[34] Wilbrink MWL, Argon AS, Cohen RE, Weinberg M. Polymer 2001; 42:10155–80.
[35] Fitt LE, Snyder EM. Photomicrographs of starches. In: Whistler RL, Bemiller JN, Paschall EF, editors. Starch chemistry and technology. Orlando: Academic Press; 1984. p. 675–89.